JACS
JOURNAL OF THE AMERICAN CHEMICAL SOCIETY
Communication
pubs.acs.org/JACS

Energy Transfer on Demand: Photoswitch-Directed Behavior of Metal–Porphyrin Frameworks

Derek E. Williams,[†] Joseph A. Rietman,[†] Josef M. Maier,[†] Rui Tan,[†] Andrew B. Greytak,[†] Mark D. Smith,[†] Jeanette A. Krause,[‡] and Natalia B. Shustova*[,†]

[†]Department of Chemistry and Biochemistry, University of South Carolina, Columbia, South Carolina 29208, United States
[‡]Department of Chemistry, University of Cincinnati, Cincinnati, Ohio 45221, United States

Supporting Information

ABSTRACT: In this paper, a photochromic diarylethene-based derivative that is coordinatively immobilized within an extended porphyrin framework is shown to maintain its photoswitchable behavior and to direct the photophysical properties of the host. In particular, emission of a framework composed of bis(5-pyridyl-2-methyl-3-thienyl)-cyclopentene (BPMTC) and tetrakis(4-carboxyphenyl)-porphyrin (H_4TCPP) ligands anchored by Zn^{2+} ions can be altered as a function of incident light. We attribute the observed cyclic fluorescence behavior of the synthesized porphyrin–BPMTC array to activation of energy transfer (ET) pathways through BPMTC photoisomerization. Time-resolved photoluminescence measurements show a decrease in average porphyrin emission lifetime upon BPMTC insertion, consistent with an ET-based mechanism. These studies portend the possible utilization of photochromic ligands to direct chromophore behavior in large light-harvesting ensembles.

Mimics of light harvesting in the natural photosystem necessitate an assembly of highly ordered chlorophyll-like chromophores for efficient light absorption with the possibility of excitation-energy funneling along a predesigned pathway. In the natural system, the high efficiency of solar energy utilization is contingent on ensemble chromophore behavior. Typically, a reaction center in a photosystem is surrounded by ~200 chlorophylls, emphasizing the utility of the molecular self-assembly process for effective design of artificial light-harvesting arrays. Such control of chromophore arrangement can be achieved in metal–organic frameworks (MOFs) through ligand-to-metal coordination.[1−5] Furthermore, MOFs show a high degree of structural and chemical tunability, imposing very few restrictions on the chromophore of choice.[3,6−10] The feasibility of using MOFs as light-harvesting antennas was recently demonstrated with porphyrin-containing frameworks, in which long-distance energy migration was detected.[11−13] In line with these studies, previous investigations of energy migration dynamics showed fluorescence quenching via metal-to-metal energy transfer (ET) in Ru(Os)-containing MOFs.[2,14−18]

Photochromic compounds capable of switching between two discrete states upon photoirradiation could be potentially utilized to control the photophysical properties of molecules coupled to the switch.[19] This approach was previously implemented in molecular donor–acceptor (D–A) dyads, in which a photoswitchable A provided control of D excited states by ET.[19,20] Those studies provided us with insight that coupling of chromophores with photoswitchable ligands could be feasible in extended structures such as MOFs. Previously, photoswitchable molecules were incorporated into MOFs to affect the porosity and gas sorption properties.[21−25] As a result of D–A pairing inside a framework, the photophysical properties of a MOF may be controlled as a function of incident light, and in particular, photoswitchable linkers could direct chromophore behavior of light-harvesting ensembles (Scheme 1). This strategy, which is a concept missing from the natural photosystem, provides the possibility of dynamic control of the ET in extended light-harvesting matrices.

Herein we prove the hypothesis shown in Scheme 1 that coordinative immobilization of a photochromic ligand, bis(5-pyridyl-2-methyl-3-thienyl)cyclopentene (BPMTC), in a porphyrin framework can direct the excited-state decay pathway of a

Scheme 1. (top) Molecular Structure of BPMTC in the Open and Closed Forms as a Function of the Excitation Wavelength; (middle) Framework 1 Constructed from H_4TCPP and BPMTC in the ON and OFF States Depending on the Wavelength of the Incident Light; (bottom) Simplified Diagram Demonstrating the Transitions Responsible for Fluorescence and Energy Transfer in 1

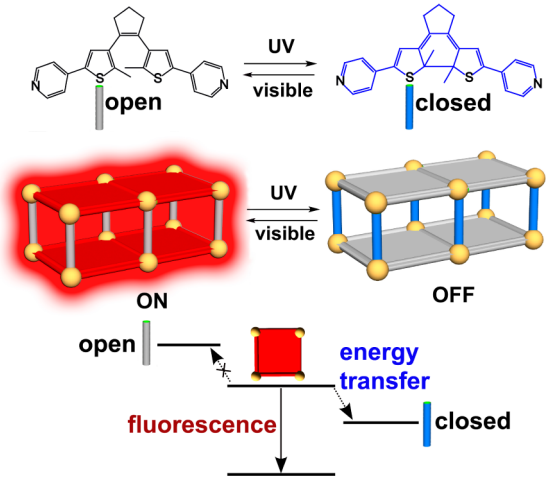

Received: June 3, 2014
Published: August 12, 2014

   dx.doi.org/10.1021/ja505589d | J. Am. Chem. Soc. 2014, 136, 11886–11889

porphyrin-based MOF. Time-resolved photoluminescence (PL) measurements were employed to monitor changes in the MOF photophysical behavior and provide estimates of the ET rate and efficiency.

Among the variety of photochromic molecules,[26] diarylethene-based compounds were chosen for immobilization inside the MOF matrix because of their fatigue-resistant photochromic performance.[27] Moreover, diarylethene derivatives are thermally stable and exhibit rapid response in the solid state.[27,28] For incorporation into a framework, a diarylethene-based core was modified with two pyridyl arms to facilitate coordination to a metal center (Scheme 1). The photochromic molecule of choice dictates the selection of the paired photoluminescent MOF, which should satisfy two main criteria. First, the emission spectrum of the MOF (D) should overlap with the absorption spectrum of the closed form of BPMTC (A) for effective resonance energy transfer (RET).[29] Second, the emissive framework should possess accessible metal sites for efficient BPMTC pillar installation. The two-dimensional (2D) framework Zn_2(ZnTCPP) [H_4TCPP = tetrakis(4-carboxyphenyl)-porphyrin] satisfies both requirements.[30] Figure 1 demonstrates

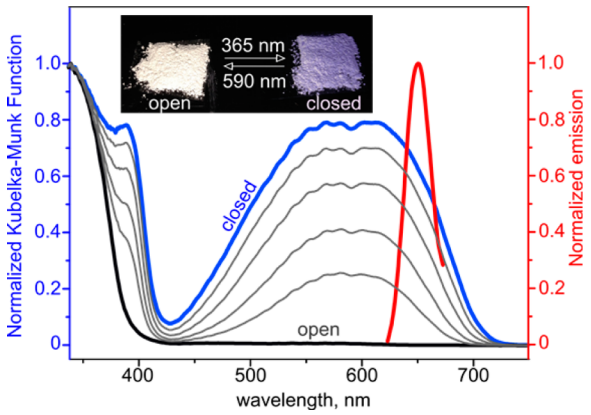

Figure 1. Diffuse reflectance (DR) spectra of BPMTC in the closed (blue trace) and open (black trace) forms, normalized to a value of 1.0 at 339 nm. Gray lines correspond to DR spectra collected during irradiation of BPMTC at 365 nm. The red trace depicts the normalized emission spectrum of Zn_2(ZnTCPP) (λ_{ex} = 590 nm). The inset shows a photograph of BPMTC after irradiation at 365 and 590 nm.

that Zn_2(ZnTCPP) is emissive in the range of 600−700 nm with an emission maximum of 652 nm (λ_{ex} = 590 nm). As a result, the fluorescence spectrum of Zn_2(ZnTCPP) overlaps with the absorption profile of BPMTC in the closed form but does not overlap with the absorption spectrum of the photoswitch in the open form (Figure 1). Thus, irradiation of the Zn_2(ZnTCPP)−BPMTC framework with UV or visible light could result in quenching or enhancement of the MOF fluorescence, respectively (Scheme 1). Furthermore, Zn_2(ZnTCPP) also fulfills the second criterion (vide supra). Its structure consists of 2D sheets made from paddlewheel $Zn_2(O_2C-)_4$ secondary building units (SBUs) bridged by $ZnTCPP^{4-}$ ligands [Figures S1 and S2 in the Supporting Information (SI)]. Each SBU contains two Zn atoms with axially coordinated solvent molecules, which can be replaced with pyridine-containing pillars.[30,31]

Before its coordinative immobilization inside a MOF matrix, the photochromic properties of the prepared BPMTC were studied in the solid state. It was found that BPMTC changed color from white to blue after irradiation at 365 nm (Figure 1), indicating conversion from the open form to the closed form. The reverse process was detected during irradiation at 590 nm. After confirmation of the solid-state photochromic behavior, BPMTC was immobilized between 2D Zn_2(ZnTCPP) layers by solvothermal synthesis (see the SI). This reaction produced red square plates of $[Zn_2(ZnTCPP)(BPMTC)_{0.85}(DEF)_{1.15}]\cdot(DEF)_{5.15}(H_2O)_{7.25}$ (**1**) (DEF = *N*,*N*-diethylformamide). The size of the obtained crystals was sufficient for single-crystal X-ray diffraction (XRD) analysis. However, several attempts using synchrotron radiation were necessary to collect a data set of sufficient quality, which to a certain extent may be explained by the photoswitchable nature of BPMTC and/or partial pillar insertion. The latter facts prevented the assignment of the residual electron density to the disordered BPMTC molecules (for more details, see the SI). However, X-ray analysis undoubtedly revealed the positions of the Zn_2(ZnTCPP) layers, and all of the C, N, and Zn atoms were refined anisotropically. As shown in Figure 2, the unit cell parameter *c* increases from

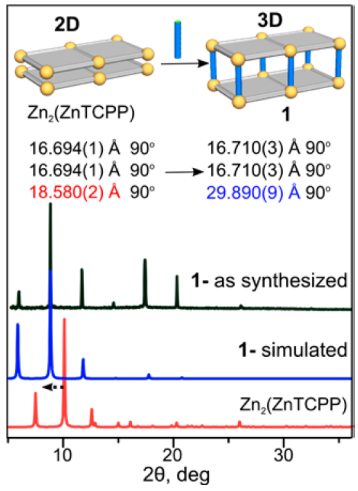

Figure 2. PXRD patterns of **1** and simulated Zn_2(ZnTCPP)[30] (preferential orientation along the 00*l* direction). The dashed arrow indicates the changes in the PXRD profile associated with the increase in the interlayer distance. The inset shows the 2D → 3D transformation by BPMTC insertion. The unit cell parameters of Zn_2(ZnTCPP)[30] and **1** were determined by single-crystal X-ray crystallography.

18.5799(15)[32] to 29.890(9) Å, indicating a change in the interlayer distance from 2.82[32] to 14.71 Å in going from Zn_2(ZnTCPP) to **1** (Figure S2). More importantly, this interlayer expansion is consistent with the size of the BPMTC pillar (Figures S2 and S3 and Table S1). Indeed, the N···N distances in BPMTC and its analogues are in the range of 14.46−15.41 Å depending on molecular conformation (Figure S2). Thereby, BPMTC bridges two Zn atoms in **1**: one Zn from a $Zn_2(O_2C-)_4$ SBU in one layer and the core Zn of a $ZnTCPP^{4-}$ porphyrin in a different layer (Figure S3). As a consequence, the pillar insertion results in a change in the layer stacking from ABAB to ABBA in going from Zn_2(ZnTCPP) to **1** but preserves a tetragonal crystal system (Figures 2 and S2 and Table S1). Notably, the pillar insertion does not affect the unit cell parameters *a* and *b*, whose values are similar in Zn_2(ZnTCPP)[32] [16.694(1) Å] and **1** [16.710(3) Å]. Powder XRD (PXRD), mass spectrometry (MS), thermogravimetric analysis (TGA), elemental analysis (EA), and ^{1}H NMR, IR, and energy-dispersive X-ray (EDX) spectroscopy were employed to study as-synthesized bulk **1** (Figures 2 and S5−S8). The PXRD pattern of **1** coincided with the simulated one from the single-crystal X-

dx.doi.org/10.1021/ja505589d | J. Am. Chem. Soc. 2014, 136, 11886−11889

ray studies (Figure 2). Comparison with the PXRD data for Zn_2(ZnTCPP) indicated a peak shift toward lower 2θ in the PXRD pattern of **1** associated with interlayer expansion and therefore BPMTC insertion. The combination of ^{1}H NMR and EDX spectroscopy, MS, and EA clearly indicated that **1** is composed of H_4TCPP and BPMTC ligands in a 1:0.85 ratio (Figures S5 and S8).

To test whether BPMTC could preserve its photoswitchable behavior after coordinative immobilization and therefore affect the photophysical properties of **1**, a sample of **1** was illuminated with light at two wavelengths, 365 and 590 nm, which drove opening and closing of the BPMTC switch, respectively. During each transition, the emission spectrum was recorded to determine relative PL intensity changes. As anticipated, irradiation at 365 nm resulted in attenuation of the PL from **1** (Figures 3 and S9) caused by BPMTC photoisomerization from

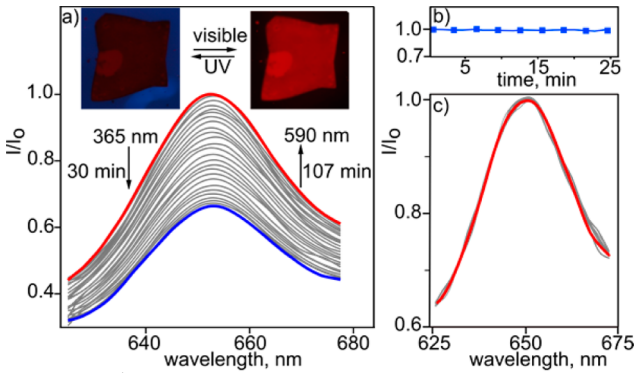

Figure 3. (a) Emission spectra recorded for **1**, scaled to give a peak intensity (I_0) of 1.0 on the first scan at λ_{ex} = 590 nm. The inset shows epifluorescence microscopy images of a crystal of **1** at λ_{ex} = 370 nm (left) and 510 nm (right). (b) Time-dependent fluorescence response of Zn_2(ZnTCPP) irradiated at 365 nm for 25 min. (c) Emission spectra recorded for Zn_2(ZnTCPP) (λ_{ex} = 590 nm) analogously to **1**. The first emission spectrum of Zn_2(ZnTCPP) is highlighted in red.

the initially open form to the closed form. We found that the fluorescence intensity was restored to the original value after irradiation at 590 nm (Figure 3). As a control experiment, the fluorescence response from Zn_2(ZnTCPP), which does not contain the photoswitchable BPMTC, was recorded at λ_{ex} = 365 and 590 nm (Figure 3). As expected, there was no enhancement or decay of the fluorescence intensity during irradiation. Furthermore, after several consecutive cycles of alternating 365 nm and 590 nm irradiation, **1** preserved its photoswitchable behavior (Figure S10). However, fluorescence decay and enhancement were observed to occur at different rates (Figure S10). For instance, a sample of **1** irradiated at 365 nm for 30 min required 107 min of irradiation at 590 nm to regain its fluorescence response (Figure 3). This fact is consistent with the photoisomerization rates that we observed for non-coordinated BPMTC in the solid state. Indeed, conversion of BPMTC from the closed form to the open form under 590 nm irradiation is ∼45 times slower than the reverse process.

To estimate the extent of fluorescence quenching accessible in **1**, the sample was irradiated for 50 min at λ_{ex} = 365 nm, which resulted in 60% modulation depth. The rate constant for fluorescence decay (I/I_0, where I_0 is the maximum of the emission intensity at 653 nm) was calculated by fitting the decay with a monoexponential function and found to be 10^{-3} s^{-1} (Figure S9). It is important to note that the PXRD analysis showed preservation of MOF integrity after sample irradiation (Figure S11), which allowed us to exclude MOF degradation as a possible cause of the changes in the fluorescence profile of **1**.

To describe quantitatively the ET processes occurring in **1**, we sought an independent measurement of the ET efficiency Φ_e based on the time-resolved fluorescence decay lifetimes (eq S1). Time-resolved decays for **1** and Zn_2(ZnTCPP) under 360 nm excitation (Figure S12) clearly demonstrated more rapid decay of **1** compared with Zn_2(ZnTCPP) over most of the acquisition time. Analysis of the curves with a reconvolution fit (eqs S2 and S3) supported triexponential decays in each case, with the longer two lifetimes moving to significantly shorter values in **1**, contributing to a shortening of the amplitude-weighted average lifetime from 1.46 to 1.24 ns, which corresponds to Φ_e = 15% and an estimated ET rate constant (k_e) of 1.2×10^{10} s^{-1}.

To address the possibility of RET in **1**, the Förster critical radius (R_0) was estimated through calculation of the spectral overlap function between the Zn_2(ZnTCPP) donor and the closed-form switch acceptor, which was found to be $J = 4.1 \times 10^{-14}$ cm^{-6} (Figure S13; see the SI for more details). Notably, the DR spectrum of BPMTC in the solid state is red-shifted in comparison with absorption in solution, and this fact was used as a rough approximation for the calculations. If this shift is included in the spectral overlap calculation, a larger estimate for R_0 results. For instance, we estimated that a 25 nm bathochromic shift leads to a 1.8-fold increase in J (Figure S13). On the basis of the calculated J, we estimated R_0 to be 30 Å (Figure S13), which is far beyond the D−A distance approximated from the structural data (e.g., the distance between Zn in the ZnTCPP unit and the corresponding N···N centroid is ∼9 Å). Therefore, RET could be responsible for the observed changes in the emission profile of **1**.

The foregoing results demonstrate that BPMTC retains photochromic properties after coordinative immobilization in a MOF matrix. The reversible response of BPMTC to optical control inputs was used to switch the emission properties of the parent framework by activation of the ET process. This system simultaneously embodies visible-light harvesting and ET governed by photoswitchable spectral overlap in an array of chromophores with well-defined distances and angles and sufficient structural integrity to permit multiple transformation cycles. This demonstrates and extends the role that a MOF can play as a versatile platform to alter[33] or preserve the ligand photophysical properties. The concept demonstrated here could foreshadow the utilization of photochromic ligands to direct chromophore behavior in large light-harvesting ensembles.

■ ASSOCIATED CONTENT

Supporting Information

Experimental details; X-ray structure refinement table and crystallographic data (CIF); NMR, MS, TGA, IR, EDX, and PXRD data; lifetime decays; and calculated spectral overlap integrals. This material is available free of charge via the Internet at http://pubs.acs.org.

■ AUTHOR INFORMATION

Corresponding Author

shustova@sc.edu

Notes

The authors declare no competing financial interest.

■ ACKNOWLEDGMENTS

N.B.S. gratefully acknowledges support from ASPIRE funding granted through the USC Office of the Vice President for Research. Crystallographic data were collected through the Service Crystallography at Advanced Light Source (SCrALS) Program at beamline 11.3.1 at the Advanced Light Source (ALS), Lawrence Berkeley National Laboratory. The ALS is supported by the U.S. Department of Energy, Office of Basic Energy Sciences, Materials Sciences Division, under Contract DE-AC02-05CH11231.

■ REFERENCES

(1) Cui, Y.; Yue, Y.; Qian, G.; Chen, B. *Chem. Rev.* **2012**, *112*, 1126.
(2) Zhang, T.; Lin, W. *Chem. Soc. Rev.* **2014**, *43*, 5982.
(3) Furukawa, H.; Cordova, K. E.; O'Keeffe, M.; Yaghi, O. M. *Science* **2013**, *341*, No. 1230444.
(4) Cohen, S. M. *Chem. Rev.* **2012**, *112*, 970.
(5) Foo, M. L.; Matsuda, R.; Kitagawa, S. *Chem. Mater.* **2014**, *26*, 310.
(6) Rosi, N. L.; Eckert, J.; Eddaoudi, M.; Vodak, D. T.; Kim, J.; O'Keeffe, M.; Yaghi, O. M. *Science* **2003**, *300*, 1127.
(7) Lu, W.; Wei, Z.; Gu, Z.-Y.; Liu, T.-F.; Park, J.; Park, J.; Tian, J.; Zhang, M.; Zhang, Q.; Gentle, T., III; Bosch, M.; Zhou, H.-C. *Chem. Soc. Rev.* **2014**, *43*, 5561.
(8) Furukawa, S.; Reboul, J.; Diring, S.; Sumida, K.; Kitagawa, S. *Chem. Soc. Rev.* **2014**, *43*, 5700.
(9) Nagarkar, S. S.; Joarder, B.; Chaudhari, A. K.; Mukherjee, S.; Ghosh, S. K. *Angew. Chem., Int. Ed.* **2013**, *52*, 2881.
(10) Leong, K.; Foster, M. E.; Wong, B. M.; Spoerke, E. D.; Van Gough, D.; Deaton, J. C.; Allendorf, M. D. *J. Mater. Chem. A* **2014**, *2*, 3389.
(11) Son, H.-J.; Jin, S.; Patwardhan, S.; Wezenberg, S. J.; Jeong, N. C.; So, M.; Wilmer, C. E.; Sarjeant, A. A.; Schatz, G. C.; Snurr, R. Q.; Farha, O. K.; Wiederrecht, G. P.; Hupp, J. T. *J. Am. Chem. Soc.* **2013**, *135*, 862.
(12) Jin, S.; Son, H.-J.; Farha, O. K.; Wiederrecht, G. P.; Hupp, J. T. *J. Am. Chem. Soc.* **2013**, *135*, 955.
(13) Lee, C. Y.; Farha, O. K.; Hong, B. J.; Sarjeant, A. A.; Nguyen, S. T.; Hupp, J. T. *J. Am. Chem. Soc.* **2011**, *133*, 15858.
(14) Kent, C. A.; Liu, D.; Ma, L.; Papanikolas, J. M.; Meyer, T. J.; Lin, W. *J. Am. Chem. Soc.* **2011**, *133*, 12940.
(15) Kent, C. A.; Mehl, B. P.; Ma, L.; Papanikolas, J. M.; Meyer, T. J.; Lin, W. *J. Am. Chem. Soc.* **2010**, *132*, 12767.
(16) Wang, C.; Lin, W. *J. Am. Chem. Soc.* **2011**, *133*, 4232.
(17) Kent, C. A.; Liu, D.; Meyer, T. J.; Lin, W. *J. Am. Chem. Soc.* **2012**, *134*, 3991.
(18) Kent, C. A.; Liu, D.; Ito, A.; Zhang, T.; Brennaman, M. K.; Meyer, T. J.; Lin, W. *J. Mater. Chem. A* **2013**, *1*, 14982.
(19) Bahr, J. L.; Kodis, G.; de la Garza, L.; Lin, S.; Moore, A. L.; Moore, T. A.; Gust, D. *J. Am. Chem. Soc.* **2001**, *123*, 7124.
(20) Irie, M.; Fukaminato, T.; Sasaki, T.; Tamai, N.; Kawai, T. *Nature* **2002**, *420*, 759.
(21) Heinke, L.; Cakici, M.; Dommaschk, M.; Grosjean, S.; Herges, R.; Bräse, S.; Wöll, C. *ACS Nano* **2014**, *8*, 1463.
(22) Luo, F.; Fan, C. B.; Luo, M. B.; Wu, X. L.; Zhu, Y.; Pu, S. Z.; Xu, W.-Y.; Guo, G.-C. *Angew. Chem., Int. Ed.* **2014**, DOI: 10.1002/anie.201311124.
(23) Park, J.; Sun, L.-B.; Chen, Y.-P.; Perry, Z.; Zhou, H.-C. *Angew. Chem., Int. Ed.* **2014**, *53*, 5842.
(24) Brown, J. W.; Henderson, B. L.; Kiesz, M. D.; Whalley, A. C.; Morris, W.; Grunder, S.; Deng, H.; Furukawa, H.; Zink, J. I.; Stoddart, J. F.; Yaghi, O. M. *Chem. Sci.* **2013**, *4*, 2858.
(25) Park, J.; Yuan, D.; Pham, K. T.; Li, J.-R.; Yakovenko, A.; Zhou, H.-C. *J. Am. Chem. Soc.* **2012**, *134*, 99.
(26) Durr, H.; Bouas-Laurent, H. *Photochromism: Molecules and Systems*; Gulf Professional Publishing: Houston, TX, 2003; p 1218.
(27) Matsuda, K.; Takayama, K.; Irie, M. *Inorg. Chem.* **2004**, *43*, 482.
(28) Matsuda, K.; Takayama, K.; Irie, M. *Chem. Commun.* **2001**, 363.
(29) Lakowicz, J. R. *Principles of Fluorescence Spectroscopy*; Springer: New York, 2007; p 980.
(30) Burnett, B. J.; Choe, W. *CrystEngComm* **2012**, *14*, 6129.
(31) Burnett, B. J.; Barron, P. M.; Hu, C.; Choe, W. *J. Am. Chem. Soc.* **2011**, *133*, 9984.
(32) Choi, E.-Y.; Wray, C. A.; Hu, C.; Choe, W. *CrystEngComm* **2009**, *11*, 553.
(33) Shustova, N. B.; Cozzolino, A. F.; Dincă, M. *J. Am. Chem. Soc.* **2012**, *134*, 19596.